Effect of electrolyte concentration on DNA A–B conformational transition: An unrestrained molecular dynamics simulation study*

Shintaro Fujimoto(藤本晋太郎) and Yu Yang-Xin(于养信)†

Department of Chemical Engineering, Tsinghua University, Beijing 100084, *China*

(Received 5 October 2009; revised manuscript received 23 December 2009)

The DNA conformational transition depends on both the DNA sequences and environment such as solvent as well as electrolyte in the solution. This paper uses the AMBER8 package to investigate the electrolyte concentration influence on the dynamics of the A→B conformational transition of DNA duplex $d(CGCGAATTCGCG)_2$. The results from the restrained molecular dynamics (MD) simulations indicate that the total energies of the systems for A–DNA are always higher than those for B–DNA, and that the A→B conformational transition in aqueous NaCl solution is a downhill process. The results from the unrestrained MD simulations, as judged by the average distance between the C5' atoms (average helical rise per ten base pair), show that the concentrated NaCl solution slows down the A→B conformational transition. This observation can be well understood by analyses of the difference between the counterion distributions around A–DNA and B–DNA.

Keywords: molecular dynamics simulation, nucleic acid, conformational transition, electrolyte

PACC: 8715B, 3620C, 8220W

1. Introduction

Deoxyribonucleic acid (DNA) is a very important substance carrying genetic information in the cells of animals and plants. When the cell needs a particular protein, the protein information written on the DNA is first copied into ribonucleic acid (RNA), and then the RNA is used directly as templates to direct the protein synthesis. A systematical investigation on DNA and RNA duplex conformation stability is helpful for us to understand their critical biological functions in the cell. Different from RNA, DNA is hydrolytically relatively stable due to its conformations.[1] The various forms of DNA have been identified as A, B, C, etc. And there have been left only five letters available to describe any new DNA structure that may be discovered in the future.[2] The physical properties of DNA sequences have been investigated extensively in Refs. [3] and [4].

It is known that A- and B-forms are two common conformations of DNA and both of them are double-stranded and right-handed helix.[5,6] The B–DNA is the dominant biological conformation of DNA in living organisms, in which two helically twisted sugar-phosphate backbones are stuffed with two types of base pair, AT and GC. The structures of A–DNA and B–DNA were well determined by the experiments such as nuclear magnetic resonance (NMR) and x–ray techniques.[7,8] There are major differences between the canonical A–DNA and B–DNA in the sugar pucker, parameters relating the base-pairs to the helical axis, the rise between base-pairs and the widths of the major and minor grooves. The preferred sugar pucker pseudorotation phase pucker value is C2'-endo ($\sim 162°$) for B–DNA and C3'-endo ($\sim 18°$) for A–DNA.[9] The A-helix is shorter and thicker than the B-helix. The helical rise of the B–DNA is 0.34 nm/bp while the A-helix is characterized by a rise of only 0.26 nm/bp.[10−12] There is a significant inclination of the base-pair plane to the axis in A–DNA, resulting in an empty channel in the centre. In addition, there is a little increase in the number of base pair per rotation and a little reduction in groove width compared to B–DNA. The minor groove width, which was measured by close interstrand phosphate distances, is 0.11 nm in A–DNA and 0.57 nm in B–DNA for the Drew–Dickerson dodecamer $d(CGCGAATTCGCG)_2$. Consequently, the major groove of A–DNA becomes

*Project supported by the National Natural Science Foundation of China (Grant Nos. 20876083 and 20736003) and Specialized Research Fund for the Doctorial Program of Higher Education of China (Grant No. 2007003009).

†Corresponding author. E-mail: yangxyu@mail.tsinghua.edu.cn

© 2010 Chinese Physical Society and IOP Publishing Ltd

deeper than that of B–DNA and the minor groove of A–DNA becomes shallower.[2,13] The A–DNA appears likely only in dehydrated samples of DNA, such as those used in crystallographic experiments, and possibly in hybrid pairings of DNA and RNA strands. Fourier transform-infrared (FT-IR) spectroscopy experiment showed that the sodium salt of the self-complementary Drew–Dickerson dodecamer persists in the B-form even the water activity is very low.[14]

Although experiments[15,16] are now able to provide accurate structures of DNA for most sequences, the analysis of large conformational changes is still a major challenge for both experimental and theoretical researchers. Taking the A–B conformational transition as an example, conformational transition depends on both the DNA sequences and environment.[17−21] Since a double-stranded DNA has two negative primary charges per base pair, both solvent and counterions provide an important role in stabilizing and in determining its overall conformation. Solvent water molecules are thought to have the function to separate charges by making use of dielectric screening and to play a conformational role in stabilizing the double helix. Counterions provide electroneutrality to a system and alleviate electrostatic repulsion between acidic phosphates of DNA by the aid of mean field effects, sequence-specific binding and water-mediated structures. To investigate more specific properties of DNA in various ion buffers, specifically Na^+ and K^+, many experimental and theoretical studies have analysed counterion condensation around DNA with respect to sequence-specific features.[22−27] The transition from B–DNA to A–DNA can be obtained *in vitro* in a few particular conditions. It is induced by equilibrating the samples under reduced relative humidity or with the increased concentration of organic solvents such as methanol,[28] ethanol[29] and trifluoroethanol.[30] It is also clear that DNA structure is very strongly influenced by the salts (electrolytes) which lead to the conversions between the distinct A–, B– and Z–DNA structural families to more local structure effects.[31,32]

Computer simulation is an alternative way to study structural properties of nucleic acid such as transformation between A–DNA to B–DNA. Since the first observation of the transition from A–DNA to B–DNA in the unrestrained molecular dynamics (MD) simulation by Cheatham and Kollman,[13] several MD simulations have shown the conformational transition of DNA in aqueous solution.[21,33−35] All the previous simulation results indicate that the A→B conformational transition is a downhill process, and that the A–DNA is not a stable conformation of Drew–Dickerson dodecamer $d(CGCGAATTCGCG)_2$ in water. Mazur observed a conformational transition from B–DNA to A–DNA by means of MD simulation, in which B–DNA in several sizes of water drop with different numbers of Na^+/Cl^- ion pairs. The results lead us to a suggestion that sodium ions bridging to phosphate strands in the major groove encourage the conformational transition from B–DNA to A–DNA.

In this paper, we perform normal pressure and temperature (NPT) MD simulations on A–DNA and B–DNA with different electrolyte concentrations using AMBER8 force fields in order to gain new insight into contribution of a wide range of electrolyte concentration on dynamics of the conformational transition from A–DNA to B–DNA. We also conducted comprehensively comparative analyses of monovalent counterion condensation around DNA and macroscopic influence of the counterions on the conformational transition.

2. Model and MD simulation details

In this section, we use Drew–Dickerson dodecamer $d(CGCGAATTCGCG)_2$ as a model DNA in the simulations, which does not lead us to the computational difficulty but can obtain reliable conclusions on A–B conformational transition preference and can diminish the influence of artificial end-effects. The 3-ns NPT ($P = 1.0$ bar and $T = 300$ K) MD simulations were performed at different NaCl concentrations (see Table 1 for particle numbers of each concentration). For each NaCl concentration four MD simulations were conducted: two for restrained DNA and two for unrestrained DNA. The AMBER8 package and PARM99 force field were used for all simulations with the periodic boundary conditions in x, y, and z directions.

Table 1. Number of particles used in the MD simulations for each system.

name of system	NaCl	H_2O	counterion
Na0	0	8154	22
Na60	60	7540	22
Na95	95	7292	22
Na110	110	7180	22

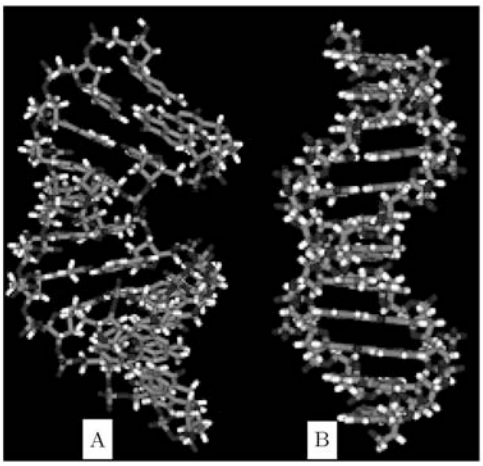


Fig. 1. Initial configurations of A–DNA and B–DNA.

The initial configurations (see Fig. 1) for all simulations were a canonical A-form or a canonical B-form of $d(CGCGAATTCGCG)_2$ built by using the programme "nucgen." To neutralize charge on DNA, we added 22 monovalent cations to the DNA, and then solvated the solute with TIP3P water, in which 22 ions and TIP3P water molecules were placed in the simulation box on the basis of Leap programme. If the system contains salt, some additional Na^+/Cl^- ion pairs were positioned in the simulation box by using Leap programme in the AMBER 8 software package after above process was finished. The size of all initial simulation boxes was set to be $62\times62\times72$ Å^3 (1 Å = 0.1 nm). The solvated systems were then optimized, thermalized and pre-equilibrated by using the MD simulation protocol shown in Fig. 2.

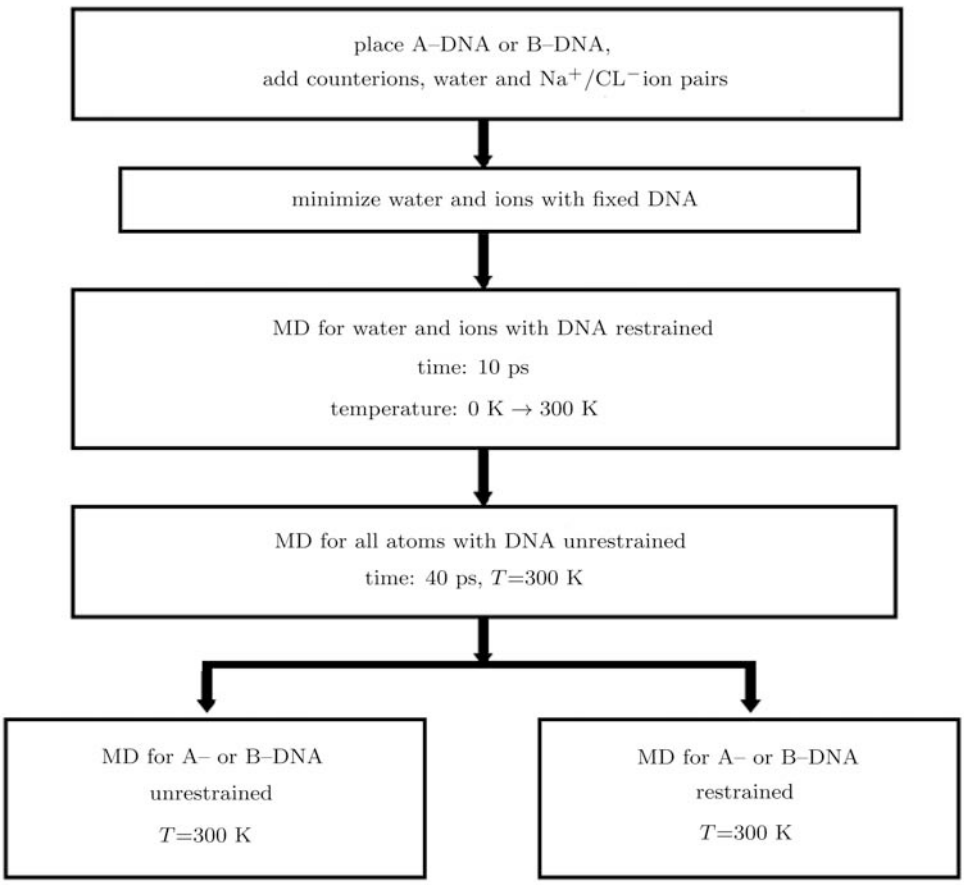


Fig. 2. The MD simulation protocol used in this work.

At the beginning of simulation, 1000 steps of minimization were performed with harmonic constraint of 500 kcal $\cdot$ mol$^{-1}\cdot$ Å^2 on the DNA, and then 2500 steps of additional minimization were performed without any constraint. At the first equilibration phase of 10 ps, each system was heated from 0 K to aimed temperature

(300 K in this work) with constraint of 10 kcal· mol^{-1}· Å^2 on the DNA. In the second equilibration phase of 40 ps, we conducted MD simulation without any constraint. The subsequent production runs were carried out for a further 2.95 ns at constant temperature by the Langevin scheme, and constant pressure (1 bar) by weak-coupling scheme. In the production run, we conducted two types of simulations. One was carried out with unrestrained DNA, and another was with restrained DNA. In the simulation with restrained DNA, DNA was restrained with a force constraint of 100 kcal· mol^{-1}· Å^2. The time step was 2 fs and all bonds involving hydrogens were constrained using SHAKE procedure. The particle-mesh Ewald (PME) procedure[36] was used to handle long-range electrostatic interactions with a non-bonded cutoff of 9 Å.

3. Results and discussion

3.1. Energies in the restrained MD simulations

We firstly conducted 3 ns restrained MD simulations for A–DNA and B–DNA at four NaCl concentrations. Figure 3 depicts the evolutions of the total energies for Na60 and Na110 systems versus time at 300 K and 1.0 bar. The total energy includes kinetic energy and potential energy of water, Cl^-, Na^+, and DNA. Drops in total energies for $t \leq 2$ ns are found in the figure and the systems reach equilibria at approximation 2 ns. The average total

Table 2. Averaged total energy for each system sampled from $t = 2$ ns to 3 ns at 300 K.

DNA	total energy $\langle E \rangle$ /(kcal/mol)			
	Na0	Na60	Na95	Na110
fixed A–DNA	−70223(18)	−77015(22)	−80887(30)	−82523(33)
fixed B–DNA	−70263(26)	−77192(26)	−81075(30)	−82690(42)
ΔE_{AB}	−40	−177	−188	−167

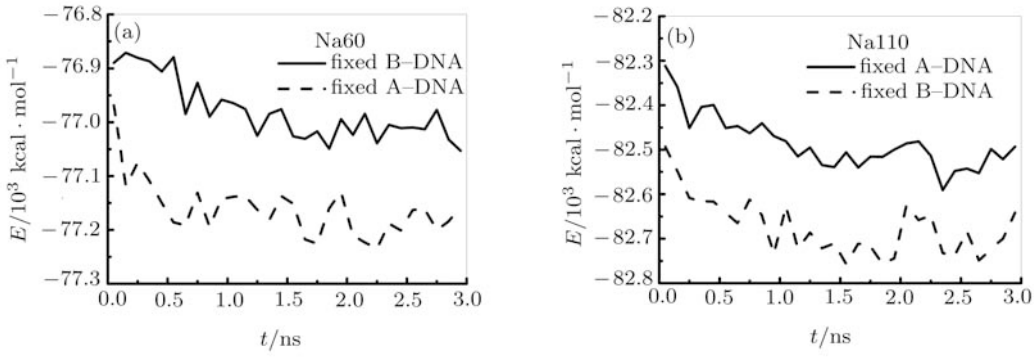


Fig. 3. Evolutions of the total energy versus time for fixed A–DNA and B–DNA in aqueous solution with different NaCl concentrations at 300 K.

energy for each system was sampled from $t = 2$ ns to $t = 3$ ns, and the results are listed in Table 2. From Table 2 one can see that the A→B conformational transition is a downhill process, and that the B-form is a stable conformation of the DNA duplex d(CGCGAATTCGCG)$_2$ in aqueous NaCl solutions. This result is in full agreement with all previous MD simulations[13,33] and experiments.[14]

We have also obtained the spatial distributions $n(r)$ of Na^+ around fixed A–DNA and fixed B–DNA in the restrained MD simulations. The spatial distribution $n(r)$ is evaluated by averaging the number of ions distributed in each coaxial cylinder with 0.05 nm thick and one-DNA turn long (2.8 nm for A–DNA and 3.4 nm for B–DNA) every snapshot. These ion distributions will help us to understand the dynamics of A→B conformational transitions of the DNA duplex d(CGCGAATTCGCG)$_2$ and the details will be given in the next subsection.

3.2. The A→B conformational transitions

The 3-ns unrestrained MD simulations are run which start from a canonical A–DNA or a canonical B–DNA as shown in Fig. 1. The simulations for Na0, Na60, and Na95 systems converge to a common structure of B–DNA within 3 ns. If we increase the simulation time, the unrestrained MD simulations for Na110 system also converge to a B–DNA structure. Figure 4 depicts the snapshots of unfixed DNA during the unrestrained MD simulations starting from the configuration of the canonical A–DNA for the Na95 and Na110 at 300 K. The length of the DNA and the inclination of base pair to axis almost changed into the canonical B–DNA at 1 ns for Na95 system. The conformation of the DNA for Na110 system are kept A–like form in the 2.95 ns production run. Nevertheless, its major grooves get larger and larger in the simulation.

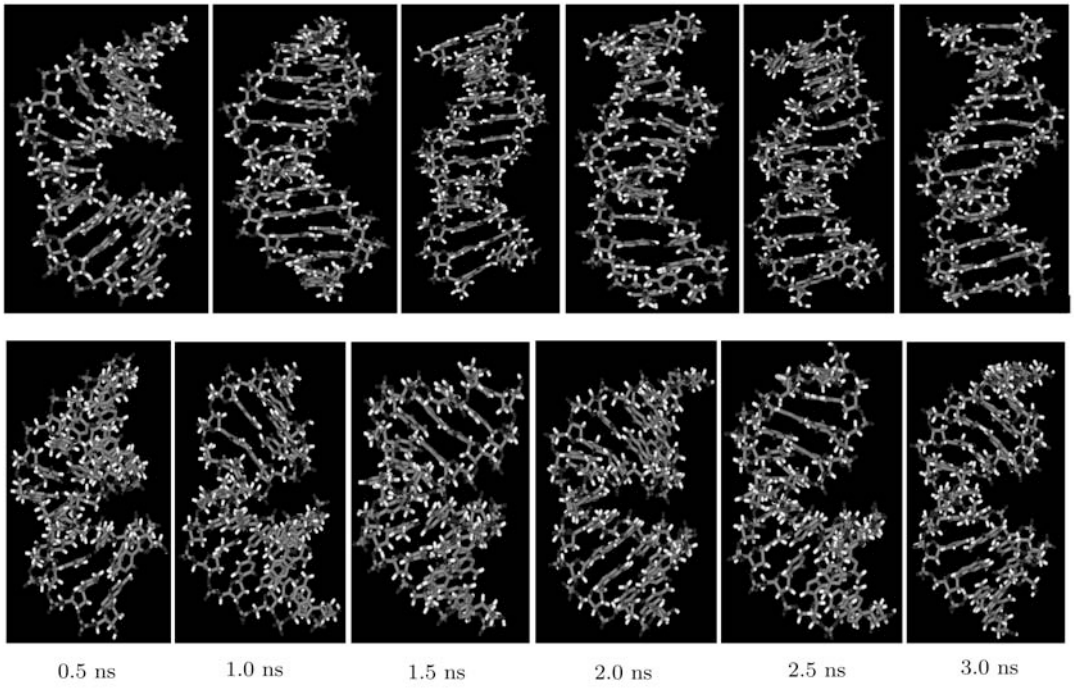


Fig. 4. Snapshots of DNA structures starting from A–DNA shown in Fig. 1 for Na95 (top) and Na110 (bottom) systems at 300 K. From left to right: 500 ps, 1000 ps, 1500 ps, 2000 ps, 2500 ps and 3000 ps.

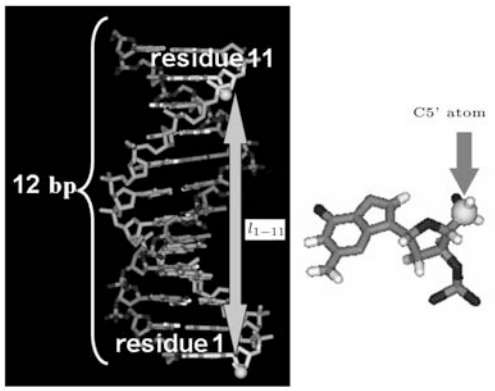


Fig. 5. Definition of the distance between C5' atoms of residues 1 and 11.

We need to compare the unfixed A–DNA with the unfixed B–DNA in the unrestrained MD simulations in terms of microscopic parameters. Nowadays DNA axis can be calculated by means of several program,[37] however, there is no defined way to evaluate the accurate DNA axis. In this work we adopt an alternative approach where the distance (helical rise) between the C5' atoms of residues 1 and 11 (l_{1-11}), residues 2 and 12 (l_{2-12}), residues 13 and 23 (l_{13-23}), and residues 14 and 24 (l_{14-24}) are used. The C5' atoms and the distance between the C5' atoms of residues 1 and 11 are shown in Fig. 5. Base pair per turn of B–DNA is 10 as well as that of A–DNA is 11, but the canonical A–DNA is much more compact than the canonical B–DNA with respect to length. In our simulation all DNA consist of the same 12 base pairs and the same sequence and thus the distance (helical rise) discussed

above is valuable for comparison of length of DNA.

Figure 6 shows the evolutions of the four distances between different pairs of C5' atoms during the unrestrained MD simulation starting from the canonical A–DNA for Na60 system at 300 K. From the figure one can see that all distances, l_{1-11}, l_{2-12}, l_{13-23} and l_{14-24}, converge to their equilibrium values simultaneously. Furthermore the equilibrium value of each distance is near 3.3 nm. This finding indicates that the average value of l_{1-11}, l_{2-12}, l_{13-23} and l_{14-24} can be used as a structural indicator for judging whether the B-form structure has been reached. The evolutions of the average distance $l_{\rm av}$ between the C5' atoms are shown in Fig. 7 for Na0, Na60, Na95, and Na110 system at 300 K. The A→B conformational transition can be clearly seen in the figures for Na0, Na60, and Na95 systems. The time for the A→B conformational transition is delayed as the NaCl concentration is increased. If we regard the time when the average distance $l_{\rm av}$ reaches 3.3 nm as the achievement of the B–DNA, the A→B conformational transition times are 0.507, 0.909, 0.954, and >3.0 nm for Na0, Na60, Na95 and Na110 systems, respectively.

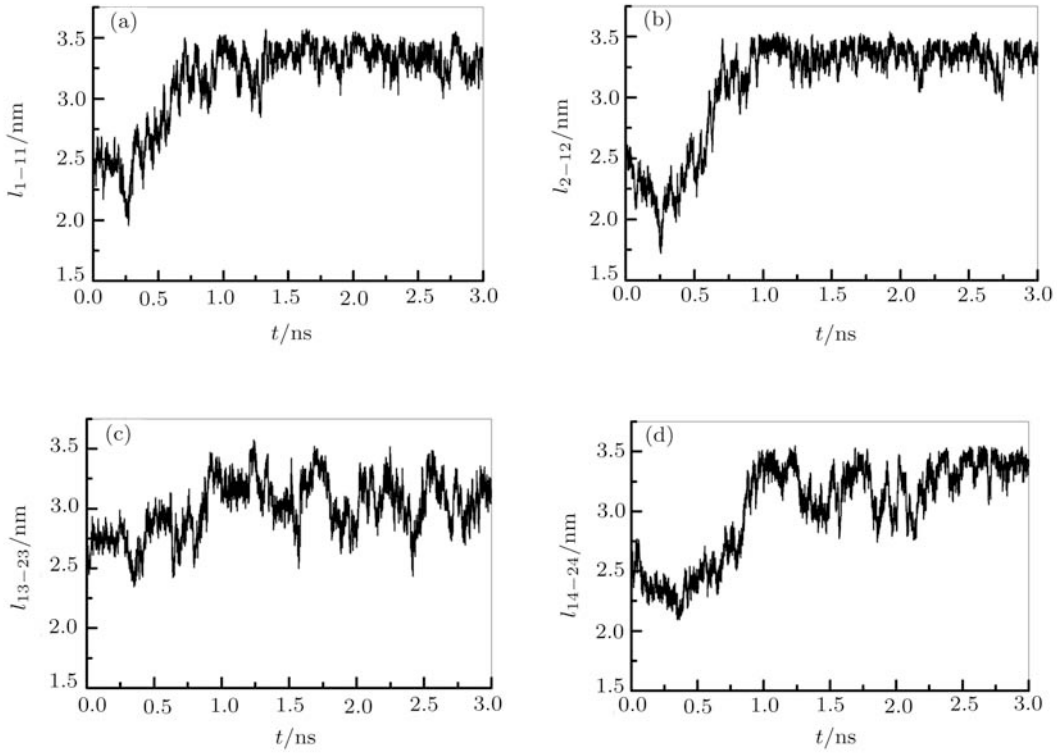


Fig. 6. Evolutions of the distances between C5' atoms during the unrestrained MD simulations starting from A–DNA shown in Fig. 1 for Na60 system at 300 K: (a) distance between residues 1 and 11; (b) distance between residues 2 and 12; (c) distance between residues 13 and 23; (d) distance between residues 14 and 24. Residues 1 to 12 are on one strand whereas residues 13 to 24 are on another strand.

The A→B conformational transition times seem to have nothing to do with the total energy changes listed in Table 2. To understand how and why concentrated NaCl solution delays the A–DNA to B–DNA conformational transition, a comprehensively comparative analysis of the ion distributions around fixed A–DNA and fixed B–DNA is made. The counterion distributions around fixed A–DNA and fixed B–DNA are compared in Fig. 8. The distributions reveal that the A–DNA first traps the Na^+ ions in its inside, and extra ions stay in its vicinity (r = 1∼1.5 nm). One can see from Fig. 8 that there is little difference among the peaks at r = 0∼1.0 nm for Na60, Na95 and Na110 systems, indicating that the major grooves of A–DNA are occupied by Na^+. The counterion distributions around the fixed B–DNA are in the different trends from those around the fixed A–DNA. No sodium ion is trapped in the centre of B–DNA (r < 0.25 nm), and most Na^+ are accumulated in

the vicinity of the B–DNA (r = 1∼1.75 nm). This is close to the distribution functions found in the previous studies.[35,38] To perform an A→B conformational transition, the counterions inside A–DNA have to move to the outside of the DNA, and therefore the counterion number inside and outside the DNA will dominate the dynamics of A→B conformational transition.

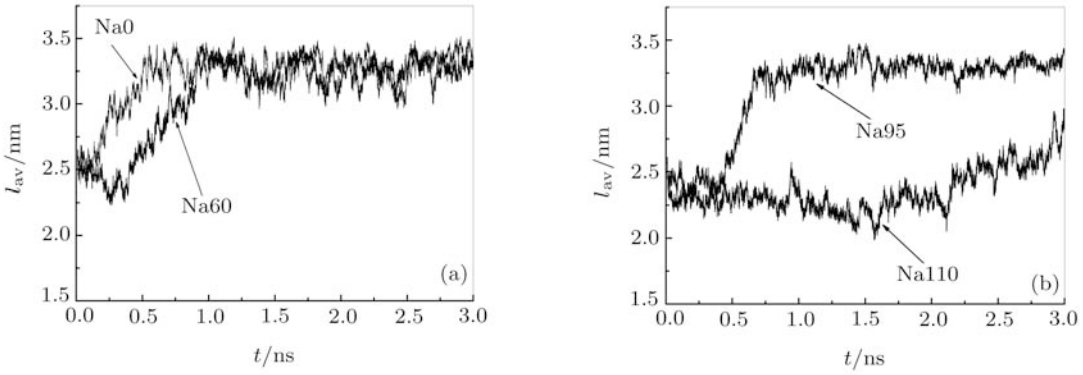


Fig. 7. Evolutions of the averaged distance among C5' atoms during the unrestrained MD simulations started from A–DNA shown in Fig. 1 at 300 K: (a) Na0 and Na60 systems; (b) Na95 and Na110 systems.

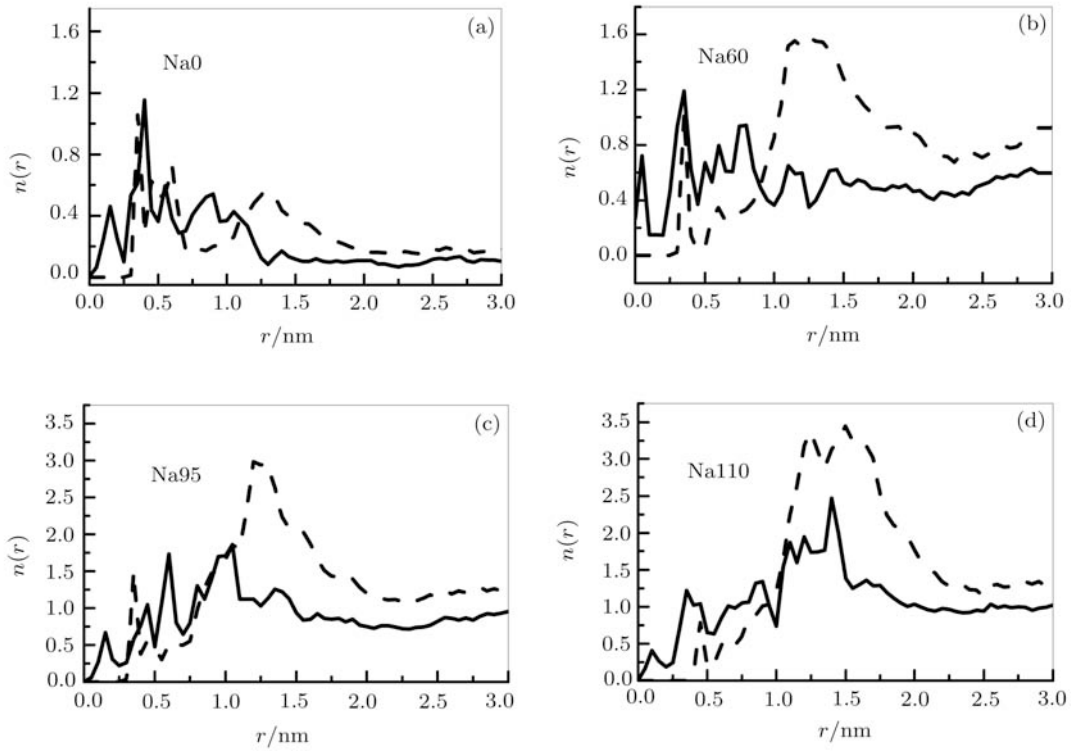


Fig. 8. Characteristic spatial number distributions of Na^+ around the fixed A–DNA (solid curves) and fixed B–DNA (dashed curves): (a) Na0; (b) Na60; (c) Na95; (d) Na110.

For convenience, we divide the counterion distribution around a DNA into three regions (layers). Layer 1 indicates the cylindrical space with the radius of 1.0 nm in which the DNA is placed in the centre. Layer 2 indicates the space around layer 1 with 0.5-nm thick, and layer 3 indicates the space around the layer 2 with 1.0-nm thick. The lengths of the cylindrical or coaxial cylindrical space used for sample correspond

to the base rises per turn of the canonical A–DNA and the canonical B–DNA. Figure 9 depicts the number of sodium ions accumulated in layer 1, layer 2 and layer 3 around fixed DNA at 300 K. Since the ions in layer 3 are located far from the DNA axis, the importance for the stabilization of DNA is relatively small. The increases of the ions in layer 1 and layer 2 for A–DNA and the ions in layer 2 of B–DNA are two key factors that influence the dynamics of the A→B DNA conformational transitions.

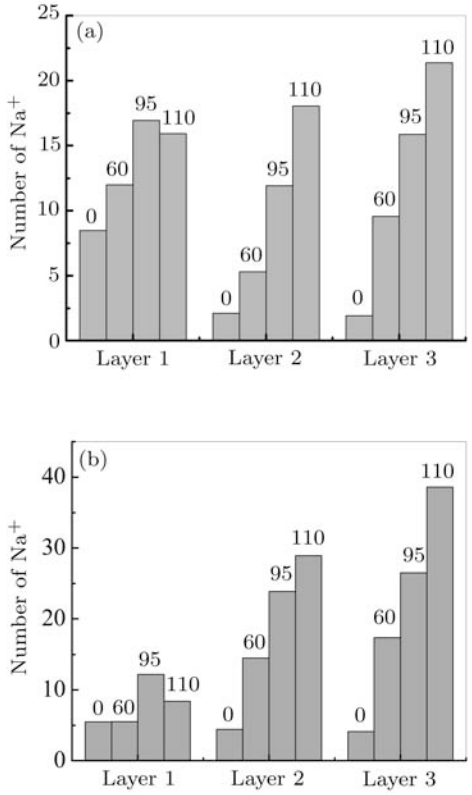


Fig. 9. The number of the ions accumulated in layer 1, layer 2, and layer 3 around (a) fixed A–DNA and (b) fixed B–DNA.

For salt free solution, the number of Na^+ in layer 1 is larger than that in layer 2 and layer 3 for A–DNA while the number of Na^+ is almost the same as that for B–DNA. In this case, Na^+ can easily move to layer 2 and layer 3, resulting in a quick conformational transition from A–DNA to B–DNA. As the NaCl concentration is increased, the number of Na^+ in layer 1 for A–DNA increases while the number of Na^+ in layer 1 for B–DNA changes very little. On the other hand, the number of Na^+ in layer 2 and layer 3 for both A–DNA and B–DNA increases dramatically. The variation difference in the number of Na^+ in layer 1 between A–DNA and B–DNA suggests that more Na^+ should move from layer 1 to layer 2 or layer 3 in the process of the A→B conformational transition, and that the increase of Na^+ in layer 2 and layer 3 makes sodium ions move towards outside layers more difficultly. This perhaps is the reason why the A→B conformational transition becomes slow in the high electrolyte concentration.

4. Conclusions

We have carried out the restrained and unrestrained MD simulations on the DNA duplex $d(CGCGAATTCGCG)_2$ in aqueous NaCl solution starting from the canonical A–DNA or the canonical B–DNA. All the MD simulations converge to a common structure of B–DNA, which is in very good agreement with previous simulation and available experimental results. The results from the restrained MD simulation at different electrolyte concentrations indicate that the total energies of the systems for A–DNA are higher than those for B–DNA, and thus the A→B conformational transition in aqueous NaCl solutions is a downhill process. As judged by the average distance between the C5' atoms, the unrestrained MD simulation results show that the increase of NaCl concentration in aqueous solution slows down the A→B conformational transition of DNA. The effect of electrolyte concentration on the dynamics of A→B conformational transition can be well understood by the counterion distributions around the A–DNA and B–DNA. With the increasing concentration of NaCl in aqueous solution, A–DNA accumulates more sodium ions in its inside and particularly in its vicinity, while B–DNA only accumulates more sodium ions in its vicinity. This difference makes the sodium ions move more difficultly from the inside of A–DNA to the vicinity of B–DNA, and in addition, number of sodium ions having to move becomes larger as the electrolyte concentration is increased. The results of this work provide a thorough understanding of concentration effect on sequence-specific structure and dynamics of the A→B conformational transition of DNA in aqueous electrolyte solutions.

Acknowledgments

We would like to thank Du Yong-Jun for her effort in preparing the manuscript. We are also very grateful to Prof. Xing Xin-Hui for his help and useful discussion on the program.

References

[1] Wang S and Kool E T 1995 *Biochemistry* **34** 4125
[2] Ghosh A and Bansal M 2003 *Acta Crystallogr.* D: *Biol. Crystallogr.* **59** 620
[3] Gao J and Xu Z Y 2009 *Chin. Phys.* B **18** 370
[4] Ma S S, Xu H, Wang H Y and Guo R 2009 *Chin. Phys.* B **18** 3591
[5] Franklin R E and Gosling R G 1953 *Acta Crystallogr.* D: *Biol. Crystallogr.* **6** 673
[6] Dickerson R E, Drew H R, Conner B N, Wing R M, Fratini A V and Kopka M L 1982 *Science* **216** 475
[7] Sheth A, Hosur R V, Govil G, Hosur M V, Kannan K K, Tan Z K and Miles H T 1989 *Biochemistry* **28** 7275
[8] Prive G G, Yanagi K and Dickerson R E 1991 *J. Mol. Biol.* **217** 177
[9] Altona C and Sundaralingam M 1972 *J. Am. Chem. Soc.* **94** 8205
[10] Fran-Kamenetskii M D 1997 *Phys. Rep.* **288** 13
[11] Wing R, Drew H, Takano T, Broka C, Tanaka S, Itakura K and Dickerson R E 1980 *Nature* **287** 755
[12] Leslie A G W, Arnott S, Chandrasekaran R and Ratliff R L 1980 *J. Mol. Biol.* **143** 49
[13] Cheatham T E and Kollman P A 1996 *J. Mol. Biol.* **259** 434
[14] Pichler A, Ruedisser S, Winger R H, Liedl K R, Hallbrucker A and Mayer E 2000 *J. Am. Chem. Soc.* **122** 716
[15] Zhao X F, Shang Y Z, Liu H L, Hu Y and Jiang J W 2008 *Chin. J. Chem. Eng.* **16** 923
[16] Li K, Dong R X, Ban G, Han H W, Su W and Yan X L 2009 *Acta Phys. Sin.* **58** 6477 (in Chinese)
[17] Ponnuswamy P K and Gromiha M M 1994 *J. Theor. Biol.* **169** 419
[18] Hagerman P J 1994 *Biochim. Biophys. Acta* **1131** 125
[19] Young M A, Rabishanker G, Beveridge D L and Berman H M 1995 *Biophys. J.* **68** 2454
[20] Borovok N, Molotsky T, Ghabboun J, Cohen H, Porath D and Kotlyar A 2007 *FEBS Lett.* **581** 5843
[21] Noy A, Perez A, Laughton C A and Orozco M 2007 *Nucl. Acids Res.* **35** 3330
[22] Savelyev A and Papoian G A 2006 *J. Am. Chem. Soc.* **128** 14506
[23] Heddi B, Foloppe N, Hantz E and Hartmann B 2007 *J. Mol. Biol.* **368** 1403
[24] Stellwagen E, Dong Q and Stellwagen N C 2005 *Biopolymers* **78** 62
[25] Wang K, Yu Y X and Gao G H 2004 *Phys. Rev.* E **70** 011912
[26] Wang K, Yu Y X and Gao G H 2008 *J. Chem. Phys.* **128** 185101
[27] Manning G S 2002 *Biophys. Chem.* **101–102** 461
[28] Vorlickova M, Minyat E E and Kypr J 1984 *Biopolymers* **23** 1
[29] Zimmermann S B and Pheiffer B H 1979 *J. Mol. Biol.* **135** 1023
[30] Vorlickova M 1995 *Biophys. J.* **69** 2033
[31] Drew H, Takano T, Tanaka S, Itakura K and Dickerson R E 1980 *Nature* **286** 567
[32] Nishimura Y, Torigoe C and Tsuboi M 1986 *Nucl. Acids Res.* **14** 2721
[33] Soliva R, Luque F J, Alhambra C and Orozco M 1999 *J. Biomol. Struct. Dyn.* **17** 89
[34] Banavali N K and Roux B 2005 *J. Am. Chem. Soc.* **127** 6866
[35] Mazur A K 2003 *J. Am. Chem. Soc.* **125** 7849
[36] Petersen H G 1995 *J. Chem. Phys.* **103** 3668
[37] Dickerson R E 1998 *Nucl. Acids Res.* **26** 1906
[38] Rueda M, Cubero E, Laughton C A and Orozco M 2004 *Biophys. J.* **87** 800